Generation and transportation of high-intensity pulsed ion beam at varying background pressures

X.P. ZHU,[1] L. DING,[1] Q. ZHANG,[1] Yu. ISAKOVA,[2] Y. BONDARENKO,[2] A.I. PUSHKAREV,[1,2] AND M.K. LEI[1,*]

[1]Surface Engineering Laboratory, School of Materials Science and Engineering and Key Laboratory of Materials Modification by Laser, Ion, and Electron Beams (Ministry of Education), Dalian University of Technology, Dalian 116024, China
[2]Laboratory of Beam and Plasma Technology, High Technologies Physics Institute, Tomsk Polytechnic University, 30, Lenin Avenue, 634050 Tomsk, Russia

Abstract

High-intensity pulsed ion beam (HIPIB) technology is developed as an advanced manufacturing method for components with improved wear, corrosion and/or fatigue performance, etc. Robust HIPIB equipment with stable repetitive operation, long-lifetime, and easy maintenance are desired for industrial applications, on which stability of ion beam parameters is critical to achieve consistent result of reproducibility. Here, magnetically insulated ion diodes (MIDs) as ion source with durable graphite anode are investigated in a simple self-magnetic field configuration under repetitive operation. Influence of background pressure on ion beam generation and transportation is emphasized since ion beam sources were intrinsically a vacuum-based system. Comparative experiments were conducted on two types of HIPIB equipment, that is, TEMP-6 and TEMP-4M, differing in vacuum packages where turbo-molecular pump or oil diffusion pump was used. Both the HIPIB equipments are operated on a bipolar pulse mode, that is, a first negative pulse of 150–200 kV with pulse duration 450–500 ns to generate anode plasma on explosive electron emission, and a second positive pulse of 200–250 kV with 120 ns to accelerate the ions. Ion beam energy density up to 8 J/cm^2 is achievable using MIDs of geometrical focusing configuration, and the total energy, energy density distribution along cross-section, deflection and divergence, and charge neutralization of the ion beams are assessed under background pressures in a wide range of two orders of magnitude, that is, 1–100 mPa. No appreciable change in the parameters is observed up to 50 mPa, and merely a slight increase in the beam deflection from about ±3 mm to about ±4 mm at the focal point over 50 mPa. The stability of ion beam at the varied pressure is mainly facilitated by the higher pressure up to several Pa in anode–cathode gap during plasma generation and good neutralizing effect for ion beam transportation.

Keywords: background pressure; explosive electron emission; high-intensity pulsed ion beam; magnetically insulated ion diode; self-magnetic field

1. INTRODUCTION

Intense particle beams, including high-power pulsed laser, ion, and electron beams offer the possibility of surface modification of components based on extreme thermal and mechanical loads to produce non-equilibrium microstructures and compound phases with fine grains in the surface layers otherwise unobtainable by traditional processing methods, especially for some hard-to-be manufactured alloys with improved wear, corrosion, and fatigue performance, etc. (Davis et al., 1996; Renk et al., 2010; Zhu et al., 2011; Chernov et al., 2014; Lei, et al., 2016). Particularly, high-intensity pulsed ion beams (HIPIB) developed in last two decades, possess some unique advantages over laser and electron beams, such as energy deposition of the highest efficiency up to 100% without beam reflection on treated surfaces frequently encountered for laser and electron beams, as well as higher specific energy density per unit volume due to the deposited energy concentrating in a thin surface layer within a few micrometers tailorable by the ion kinetic energy and ion species (Bystritski & Didenko, 1989; Rej et al., 1997; Renk et al., 2004; Remnev et al., 2014). Due to the high efficiency of ion beam–matter interaction, significant coupled thermal and mechanical loads could be obtained under HIPIB irradiation at a beam power/energy

density output per pulse of 1–2 order lower than that of laser and electron beams. Typical HIPIB parameters for surface modification of components are in the range of energy density 1–10 J/cm^2 under ion accelerating voltage of 100–400 kV in pulse duration typically of 10 ns–1 μs, causing intense heating and cooling at a rate of higher than 10^9 K/s in the near-surface layers of 0.1–10 μm of irradiated materials. For instance, ion beam shock processing is thus obtainable in a non-confinement regime at a moderate power density of 10^7–10^8 W/cm^2, resulting in surface hardening/strengthening down to a subsurface layer of hundreds micrometers for metallic and ceramic components under the HIPIB irradiation (Lei et al., 2009; Zhu et al., 2014). In addition, HIPIB output at a higher power/energy density is applicable for high-rate deposition of functional thin films by ablation of solid targets at room temperature (Suematsu et al., 2002; Zhu et al., 2008). Therefore, the HIPIB technology for surface modification relies on microstructures and/or compounds far from equilibrium states due to strongly coupled thermal and dynamic effects under the beam–material interactions, greatly distinguished from conventional ion implantation technique mainly based on alloying and doping effects.

Magnetically insulated ion diodes (MIDs) have been intensively investigated since the last three decades and are still recognized as the most efficient type of high-power ion source for high-intensity pulsed ion beam generation (Bystritski & Didenko, 1989; Rej et al., 1993; Werner et al., 2001; Zhu et al., 2002). Note that, for HIPIB practical applications, it is necessary to provide high reproducibility of its parameters on the irradiated targets. Stability of HIPIB parameters in a series of repetitive pulses is involved with not only the amplitude and shape of accelerating voltage pulse from pulsed power sources applied to ion diodes, but also the ion beam energy distribution along axis and cross-section direction upon ion beam transportation and propagation in vacuum. It is well known that, conventional ion implanter with ion current up to mA range is commonly operated under a low background pressure of 1 mPa order with long mean free path for ion transportation to achieve high-current implantation of reproducible parameters for surface modification of materials (Lei et al., 2002). The HIPIB source of ion diodes is also intrinsically vacuum-based system, nevertheless, it could be extended to a wider application if it is robust and tolerant under low or medium vacuum conditions of the background gaseous pressures due to variations in processing conditions such as degradation of ion source material itself, gaseous release from either ion source material or processed components, or introducing reactive gases puff into the processing chamber during HIPIB irradiation for materials processing. Thanks to the short pulse high-current discharge process of HIPIB generation as well as its unique modification principle of high-energy density ion–matter interaction other than that of alloying element incorporation highlighted in conventional ion implantation, it is feasible for the HIPIB technology to utilize discharge and transport

at a higher background pressure. It was reported in some previous studies that a large flux of energetic neutrals in the ion beam may be produced by MIDs (Pointon 1989; Pushkarev et al., 2015). The neutrals are generated through charge exchange processes between the ions and background gas molecules in anode–cathode (A–K) gap. The charge exchange in an ion diode is actually beneficial to overcoming the limitation of space-charge effects in the A–K gap for intense ion beam extraction. And the energetic neutrals of the complex beam also contribute significantly to enhancement in the HIPIB energy density. As a result, the energy density per shot could be enhanced by a factor of 25–30 as compared with the space-charge-limited value (one-dimensional Child-e–Langmuir limit) (Pushkarev et al., 2015). Moreover, the standard deviation of HIPIB energy density in a series of pulses does not exceed 11%, whereas the corresponding variation of ion current density was 20–30% (Pushkarev et al., 2014). The improved stability of energy density from pulse to pulse is thought to be associated with the generated energetic neutrals from the charge exchange between accelerated ions and background gas molecules.

However, it was reported that the volt–ampere characteristics of ion diode and ion beam energy did not depend on the background pressure within the range of 2.6–1300 mPa (Stepanov et al., 2008), where an annular MID with a dielectric anode in a B_r magnetic field was operated at diode voltage of 400 kV and pulse duration of 60 ns. It was also found that, the pressure in the vacuum chamber increased at the expense of decomposition and/or decontamination of the dielectric material on anode surface, and the amplitude of pressure increase varied within a range 27–133 mPa during a series of repetitive pulses. The pressure within A–K gap is estimated to be up to 100 Pa during a pulse, taking into account the volume of diode chamber of 0.25 m^3, the effective anode surface area of 200 cm^2 and the A–K gap distance of 1 cm. Therefore, in that case, the background pressure in diode chamber between pulses up to 1300 mPa could have a negligible influence on operating mode of the ion diode. Nevertheless, some unfavorable phenomenon, for example, breakdown of coils powered with pulsed voltage of 5–10 kV for generating a magnetic field or surface flashover in chamber wall, occurred more frequently as the chamber pressure increased, causing unstable operation of the diode system. On the other hand, change of background pressure in diode chamber also affects HIPIB transportation to a target. The ion beam transportation process was studied previously for ion diodes of different types (Olson 1982), and it was shown that MIDs have a maximal HIPIB divergence of 1°–4° (ratio of HIPIB spot radius at half-height to the distance from the diode), unobtainable in reflex diodes and pinch diodes. When an ion beam is injected into neutral gas, the gas will be ionized and stripped to some equilibrium charges, and a portion of the ions in the HIPIB will lose their kinetic energy due to induced electric fields and inelastic collisions, creating a plasma distribution that facilitates neutralization of the ion beam. In the self-pinched mode, the ion

beam ionizes the gas and creates a highly conductive plasma channel during the initial period of the beam pulse. Self-pinched transport of intense ion beams in low-pressure background gases was also studied for ion-driven inertial confinement fusion using numerical simulations, where the self-pinched transport of intense proton beams of MeV range produced on Gamble II (1.5 MeV, 100 kA, 3 cm radius) is expected to occur at gas pressures 4–10 Pa of He or 0.4–1.3 Pa of Ar (Rose et al., 1999).

Despite many researches were carried out to study influence of background gases pressure in diode chamber on HIPIB generation and transportation, there are no experimental investigations on MIDs with self-magnetic insulation. Especially, it is still not practical to define optimum pressure of residual gases in diode chamber of HIPIB equipment for surface engineering applications where the moderate kinetic energy of ions is preferably in hundreds keV for more effective depositing of the beam energy in the top surface layer of processed components. In recent studies, stability of HIPIB generation in a series of pulses for strip ion diodes of self-magnetic insulation mode are presented at a low pressure in diode chamber about 10 mPa (Pushkarev et al., 2014). In this study, influence of background pressures varied in the two order of magnitude of 1–100 mPa on ion beam characteristics is comparatively studied for self-magnetic field MID with graphite anode on two HIPIB sources differed in vacuum system, toward a general understanding of stability of HIPIB parameters at varying background pressures for HIPIB technological equipment development.

2. EXPERIMENTAL

2.1. HIPIB equipment

HIPIB generation from MIDs with self-magnetic insulation were carried out on two ion accelerators, TEMP-6 (Zhu et al., 2002) and TEMP-4M (Pushkarev et al., 2013), having similar pulsed power design of a microsecond pulsed voltage generator (Marx generator) and a nanosecond pulsed voltage generator (double coaxial pulse forming line, PFL). During operation, the PFL is charged by Marx generator, and then a bipolar pulse is output from the PFL through impedance-matched transmission line to the MIDs, where the first negative pulse with peak voltage of 150–200 kV lasting 480–500 ns for explosive emission plasma formation and the second positive one of 200–250 kV with pulse duration of 120 ns for HIPIB extraction. In order to enhance electrical efficiency, the charging inductor in previous PFL design (Zhu et al., 2002) has been removed to eliminate current leakage through it. As a result, the energy delivery from the PFL to the diode is increased by a factor of 1.5 that in turn stabilizes to some extent the anode plasma formation process. Moreover, to improve the statistical stability of PFL output for the bipolar pulse with an accurate delay time, the PFL gas switches previously operated in self-breakdown of N_2 and SF_6 mixtures at a pressure range within 1.5–3.0 atm

(Zhu et al., 2002) have been modified with a passive external triggering circuit connecting from the output switch to the reverse switch (the main spark gap) of PFL, by which the reverse switch is externally started by a triggering pulse transformed from a voltage divider near the output switch during output of rising front of the first negative pulse., the delay time of bipolar pulse, that is, duration of the first negative pulse in the present case, can be precisely controlled with a jitter no more than ±10 ns predefined by the length of coaxial cable in the passive triggering circuit connecting the two PFL switches. In this newly upgraded PFL setup, the gas switches can be filled with pure N_2 at a higher pressure up to 6 atm, and an optimal delay time of 480–500 ns is determined for the present study.

2.2. Characterization of accelerator and HIPIB parameters

The diode voltage was measured with a voltage divider installed on the impedance-matched transmission line between the PFL output switch and the diode unit, and the diode current was measured using a Rogowski coil just behind the transmission line. Electrical signals from the sensors were recorded with a Tektronix DPO 2024B oscilloscope (200 MHz, 1×10^9 sampling/s). The diode units and typical waveforms of diode voltage and current are presented in Figure 1. The anode is made from graphite having a focusing curvature of 15 cm.

HIPIB total energy and energy density distribution in cross-section were measured by employing an infrared (IR) diagnostic method (Pushkarev et al., 2015). This method enables the beam energy measurement of high spatial resolution (1 mm) and high sensitivity (0.01–0.02 J/cm^2). A typical thermal imprint recorded by the IR camera 100 ms after one pulse irradiation onto a stainless steel target (thickness of 0.1 mm) is illustrated in Figure 2, together with energy density distribution along the ion beam cross-section vertical and horizontal lines indicated in the thermal imprint. The thermal imprint of the beam was recorded through a barium fluoride (BaF$_2$) window, located on the flange of the diode chamber. This method was calibrated before measurement since the BaF$_2$ window has incomplete transmission in spectral range of 7–14 μm for the IR camera used in this study.

The energy density measurement experiments have been carried out in two setups, that is, with/without attenuation of an ion beam. In the attenuation setup, two grids made from stainless steel with a transparency of 60% each are placed respectively on the positions of 5 and 10 cm downstream from the A–K gap, producing a total attenuation value being 36% of original ion beam energy density. In two setups, A–K gap and accelerating voltage for HIPIB generation are kept unchanged. The background pressure of ion diode chamber is adjusted in a range of 1–100 mPa by controlling the opening of vacuum valves in the main chamber of the HIPIB equipment, where TEMP-6 is composed of mechanical pump and turbo-molecular pump, and TEMP-4M has mechanical pump and oil diffusion pump without a nitric trap. Therefore, the major residual gaseous species in
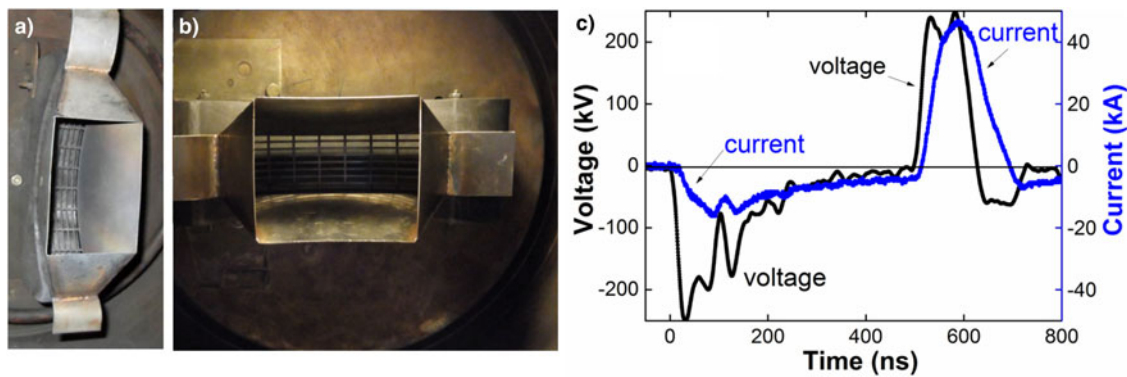
Fig. 1. Ion diodes of self-magnetic field insulation in two accelerators and typical waveforms of accelerating voltage and total diode current: (a) MID in TEMP-4M, (b) MID in TEMP-6, (c) waveforms of voltage and current.
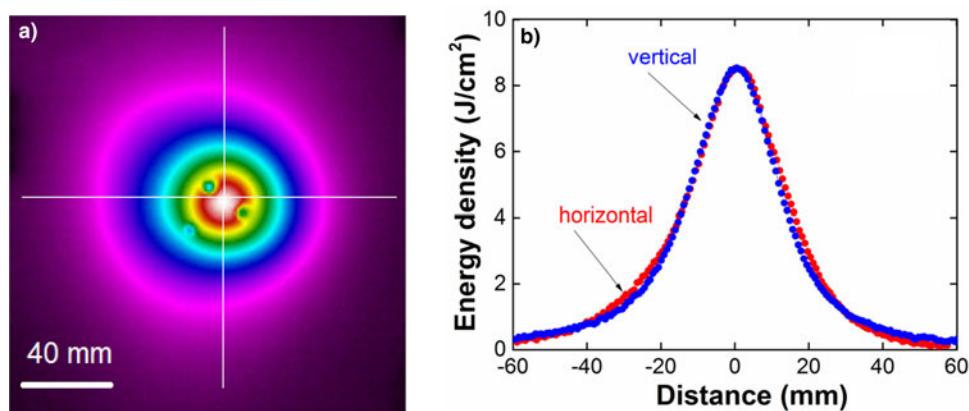

Fig. 2. Infrared (IR) diagnostic method: (a) typical IR image of the ion beam spot imprint on a thin foil metal target, (b) the beam energy density distribution along the cross-section vertical and horizontal lines indicated in (a).

TEMP-6 are nitrogen and oxygen molecules, while TEMP-4M has residual oil vapor in addition to the residual nitrogen and oxygen molecules. Ion beam total energy, energy density distribution in cross-section, ion beam deflection and divergence, and ion beam charge neutralization are analyzed with respect to variations in background pressure.

3. INFLUENCE OF VACUUM CONDITIONS ON HIPIB PARAMETERS

3.1. HIPIB energy density and total energy

Figure 3 shows the HIPIB total energy and energy density in focus point of ion beam are presented in series of shots with a continuous change in background pressure in diode chamber. A stainless steel foil target (thickness of 0.1 mm) was placed at the focus with a distance of 15 cm to the cathode. In this series of experiments, the HIPIB energy density has been measured directly without attenuation of ion beam in a series of pulses and a polynomic curve is fitted to show the changing tendency of ion beam energy density. Figure 4 shows the HIPIB total energy and energy density vs. background pressure in series of shots measured with ion beam

attention scheme by using two grids placed in front of the ion diode. In this case, the ion beam energy can be more accurately evaluated as a result of no surface ablation.

The maximum HIPIB energy density measurement by IR diagnostics is limited by evaporation of a target material (Davis et al., 1997). For a stainless steel target, the upper limit of energy density measurable by IR-diagnostics is $3.5\text{–}4\,\mathrm{J/cm^2}$. It is found that, after attenuation of an ion beam by two grids the target was heated up to a temperature slightly lower than that of target irradiated by ion beam without attenuation. Therefore, the HIPIB energy density and total energy without grids on the cathode can be estimated by taking into account a correction factor $K = 2.8$ for the two grids that led to a final transparency of 36%. Figure 5 shows the results of statistical measurements of HIPIB energy and energy density at a background pressure of 3–5 mPa in diode chamber. Variation of HIPIB energy and energy density at the constant pressure is about 6% (standard deviation), comparable with that of a series of pulses with varied background pressure within 1–100 mPa. Therefore, it is revealed that, insignificant decrease in HIPIB energy density with background pressure growth in the diode chamber confirmed by both modes of energy density measurements of with/without attenuation.
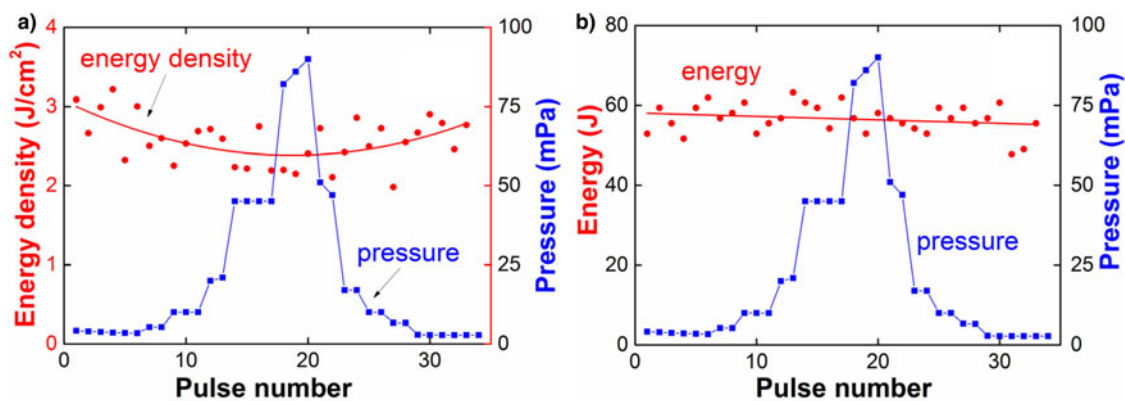
Fig. 3. Shot-to-shot variation in the HIPIB energy density and total energy vs. background pressure in a series of pulses measured directly that led to an underestimated value due to surface ablation on the target: (a) energy density, (b) total energy.
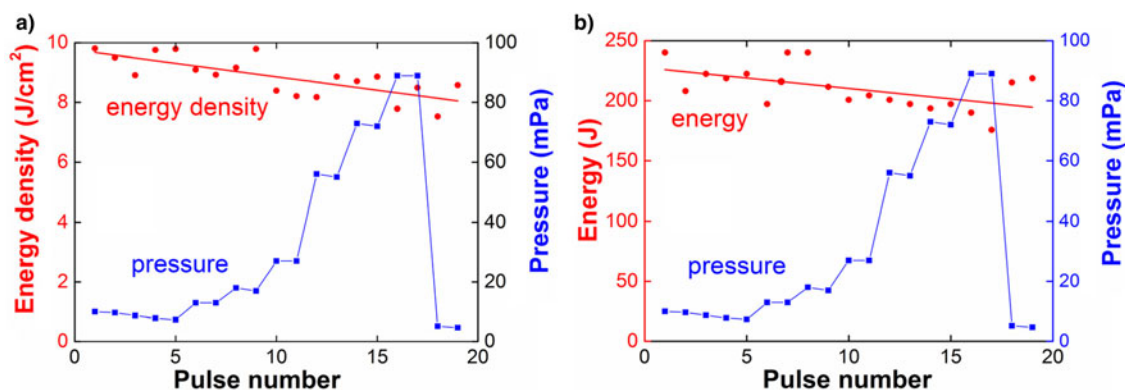

Fig. 4. Shot-to-shot variation in the HIPIB energy density and total energy vs. background pressure in a series of pulses with measurement scheme of attenuation: (a) energy density vs. pressure, (b) total energy vs. pressure.

3.2. HIPIB deflection

To evaluate the influence of vacuum conditions on HIPIB transportation, ion beam deflection was recorded to monitor the movement of ion beam spot center (i.e., the point of the maximum energy density on the IR image) on the target in
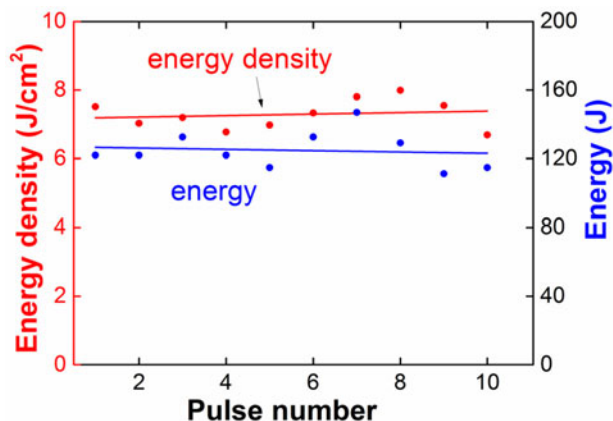

Fig. 5. Shot-to-shot variation in HIPIB energy density and full energy at a background pressure of 3–5 mPa.

focus in a series of pulses. Three holes in diameter of 3 mm were made on the stainless steel foil target (Fig. 2), for positioning the ion beam center movement. Figure 6 shows deviation of ion beam center position with respect to change of background pressure in diode chamber, where the beam center position denotes the distance between the HIPIB spot center and one of the three holes along vertical direction.

Moreover, the HIPIB deflection at a constant vacuum was assessed for comparison purpose. Figure 7 presents the result of HIPIB deflection at the high-energy density output of 7–8 J/cm², at a background pressure of 3–5 mPa in diode chamber. In this case, both vertical and horizontal movements were counted. It is shown that, moving of the HIPIB spot has little change in series of pulses as the background pressure in diode chamber is varied within 1–100 mPa. At a constant vacuum condition of 3–5 mPa, moving of the ion beam spot in series of pulses is no more than ±3 mm, and at a background pressure higher than 50 mPa, a slight increase in the beam deflection was observed, not exceeding ±4 mm. The slight increase could be attributed to increased probability of surface breakdown of the insulator and/or the breakdown of the residual gas in the diode chamber at the pressure higher than 50 mPa. In some cases, abnormal
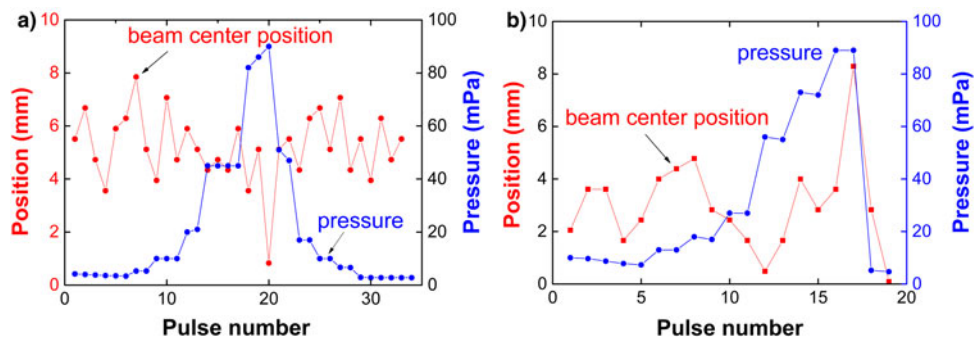
Fig. 6. Shot-to-shot variation in the ion beam deflection in vertical direction and background pressure in diode chamber: (a) low-energy density output at 3–4 J/cm^2, (b) high-energy density output at 7–8 J/cm^2.
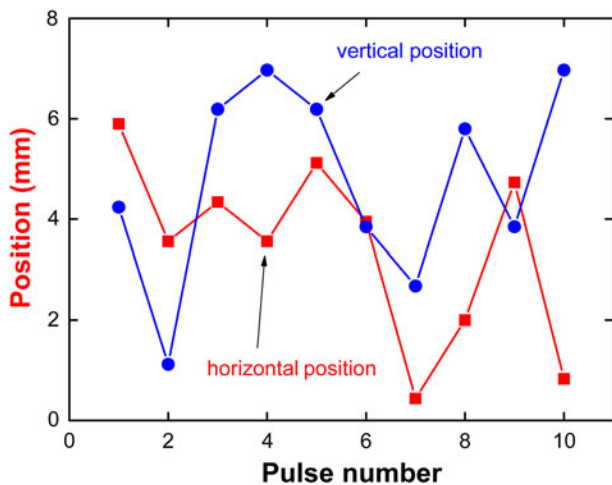

Fig. 7. Shot-to-shot variation the ion beam deflection in horizontal and vertical direction at a vacuum of 3–5 mPa.

discharge could occur, such as a bright glow on the surface of the polymeric insulator leaving breakdown traces on the surface, and the corresponding total current increases abruptly.

3.3. HIPIB divergence

The HIPIB transportation characteristics were also assessed by the distribution of beam energy density in the focal plane. It is found that, variation in background pressure within 1–100 mPa has little influence on the HIPIB energy density profile in the focal plane, merely leading to slight expansion of ion beam cross-section and variation in the peak value of energy density is indistinguishable (Fig. 8). To compare the divergence of HIPIB energy density distribution at different background pressure in the chamber, the horizontal cross-section is chosen on the right hole of the target (Fig. 2). Figure 9 shows the results of ion beam divergence, defined as the ratio of the beam radius at half-height to the distance from the diode, in a series of pulses. Change of HIPIB divergence in a series of pulses has been approximated by using a straight line at least-squares method. The divergence in series of pulses was about 5.6° ± 8%, being independent on the background pressure in diode chamber.

3.4. HIPIB full charge

It is known that a strong electric field established in intense ion beams can causes their scattering along the length of ion propagation (Bystritski & Didenko, 1989). Therefore, ion beam scattering may be mitigated or eliminated by reducing the beam-generated electric field through mixing low-energy electrons into the ion beams, that is, charge neutralization of ion beam. To evaluate the ion beam charge neutralization effect, we employed a charge collector
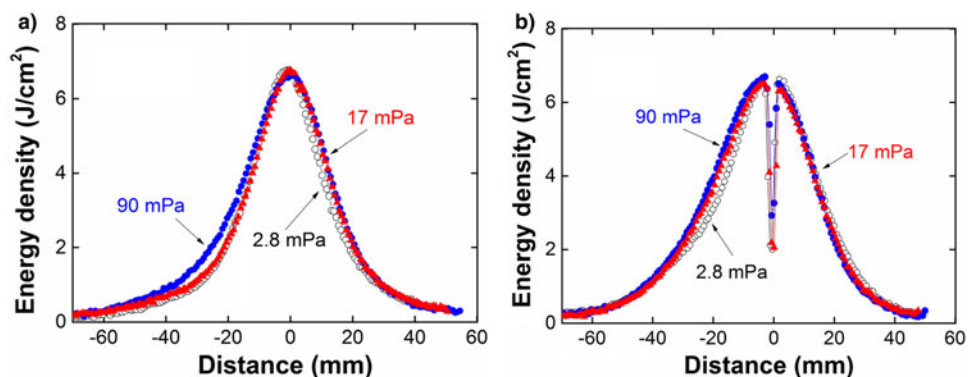

Fig. 8. Profiles of HIPIB energy density in the focal plane along the two directions: (a) vertical direction; (b) horizontal direction, respectively, at the different background pressures in diode chamber.
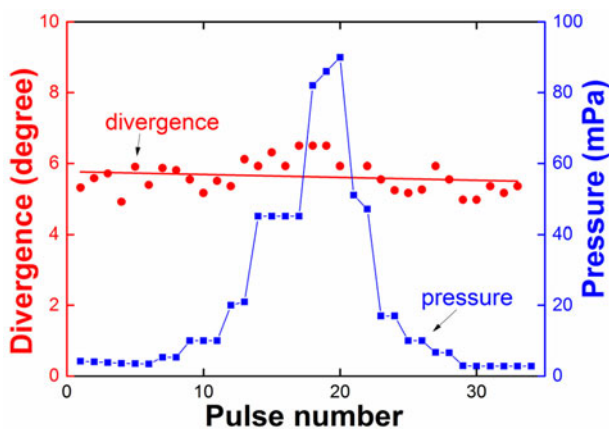
Fig. 9. Shot-to-shot variation in the ion beam divergence in vertical direction vs. background pressure in diode chamber, at low HIPIB energy density regime (3–4 J/cm^2).

without using magnetic field and voltage bias to receive both ions and electrons of neutralized beam. The diameter of the collector was 8 mm and the diameter of the entrance hole was 4 mm. The charge collector was located at the focus, 15 cm downstream from the diode. The waveforms of accelerating voltage, ion current density and neutralized beam current density are shown in Figure 10, respectively.

Ion current density was measured using a magnetically insulated Faraday cup ($B = 0.4$ T) for cutoff of electrons. Time-of-flight analysis of the HIPIB composition is performed on the measured ion current density (Figure 10). In the space-charge-limited mode, taking into account expansion of anode plasma, the ion current density can be described as follow according to the Child–Langmuir relation (Langmuir, 1913):

$$J_{ion} = \frac{4K\varepsilon_0\sqrt{2z}}{9\sqrt{m}} \cdot \frac{U^{3/2}}{[d_0 - v(t - t_0)]^2}, \quad (1)$$

where d_0 is the initial A–K gap, ε_0 the absolute permittivity of vacuum, v the plasma expansion rate, m the ion mass, z the ion charge, t_0 the time in a bipolar pulse and at the moment the polarity on the potential electrode reverses $t_0 = 500$ ns (Fig. 10), and K amplification coefficient of ion current density over the Child–Langmuir limit.

Note that, the calculated values of ion current density on Eq. (1) have been increased for illustration considering the effect of HIPIB focusing on the ion current density enhancement. The enhancement factor is constant during pulse of accelerating voltage and estimated to be of a value of $K_H = 2$ for protons and $K_C = 40$ for C^+ ions, respectively. According to the results of ion beam space-charge compensation measurements, the concentration of neutralizing electrons in the focus exceeds the ion concentration by a factor of 1.1–1.2. The electrons energy does not exceed 50 keV. Figure 11 shows the charge density of HIPIB vs. background pressure in diode chamber in a series of pulses, calculated by integrating the neutralized beam current density at 550 ns $< t < 750$ ns (Fig. 10). Increase in background pressure in diode chamber slightly enhances the negative charge of electrons, and thus it is indicated that the variation of pressure will not essentially alter the process of HIPIB charge neutralization.

3.5. Change of residual gas in diode chamber

Some comparative experiments on influence of vacuum conditions on HIPIB generation and transportation were carried out on accelerator TEMP-4M. Figure 12 shows the photograph of the focusing diode and HIPIB thermal imprint recorded on the target in the focal plane with a distance of 14 cm from the diode.

Figure 13 shows the results of statistical measurements of total diode current and HIPIB energy density at a background pressure of about 10 mPa in diode chamber, respectively. The pulse repetition frequency was six pulses per minute for total current measurement, and one pulse in 2 min for HIPIB energy density. The standard deviation of the
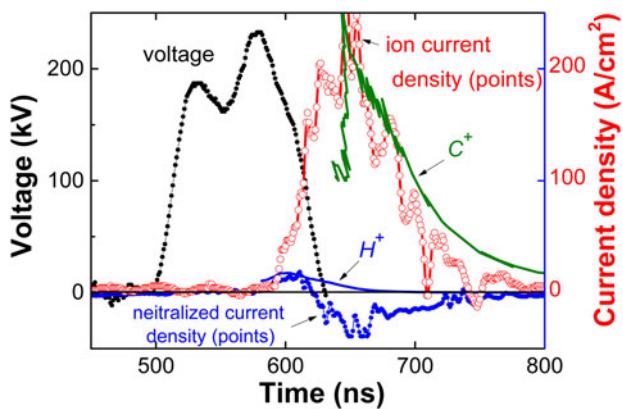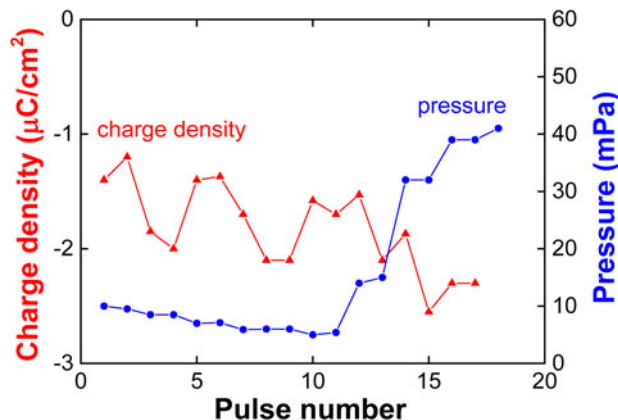

Fig. 10. Waveforms of the accelerating voltage (second pulse), ion current density, and neutralized beam current density that is measured by a charge collector covered with a 10 μm Al foil, and calculated ion current density of protons and carbon ions is also presented.

Fig. 11. Shot-to-shot variation in the ion beam charge density vs. background pressure in diode chamber.
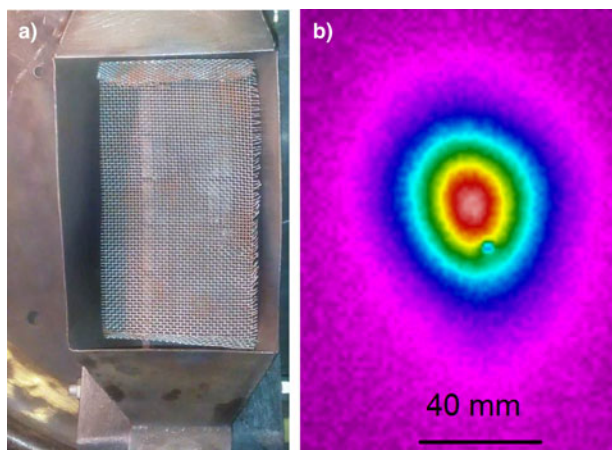
Fig. 12. Photograph of the MID on TEMP-4M and infrared (IR) image for energy density measurement: (a) strip focusing diode with attenuation metal mesh installed at the output of the focusing diode, 5 cm downstream from the cathode; (b) an IR image of the beam on a target at focus point, 14 cm downstream from the diode.

energy density was 6–7% and at the same time the variation in total current was 2–3%. Figure 14 presents the results of ion beam deflection in a focal plane in a series of pulses at the background pressure of about 10 mPa. Moving of the

HIPIB center in a focal plane did not exceed ±3 mm, with a standard deviation of 1.3 mm in the vertical direction and 0.6 mm in the horizontal direction.

4. DISCUSSION

On the experimental data presented in this study, the effect of the background pressure on the stability of HIPIB parameters can be dealt with by concerning the ion beam generation (anode plasma generation) and transportation. The ion beam generation in the MIDs with self-magnetic insulation in the bipolar pulse mode is largely defined by processes in A–K gap during variation in the background pressure. It is estimated that, before anode surface explosive emission during the negative pulse, the adsorption of residual gas onto anode and cathode surface may lead to a superficial density at least of 10^{15}–10^{16} cm^{-2} even merely considering several monolayers of residual gas molecules adsorbed on (diameter of molecules N_2 and $O_2 \approx 3$ Å). These molecules are readily desorbed by explosive plasma formation at the anode and cathode surface. At explosive emission, plasma expansion rate (and corresponding speed gas layer expansion) is about 1–2 cm/μs during the first negative pulse with a duration of 400–500 ns, and thus the density of neutral
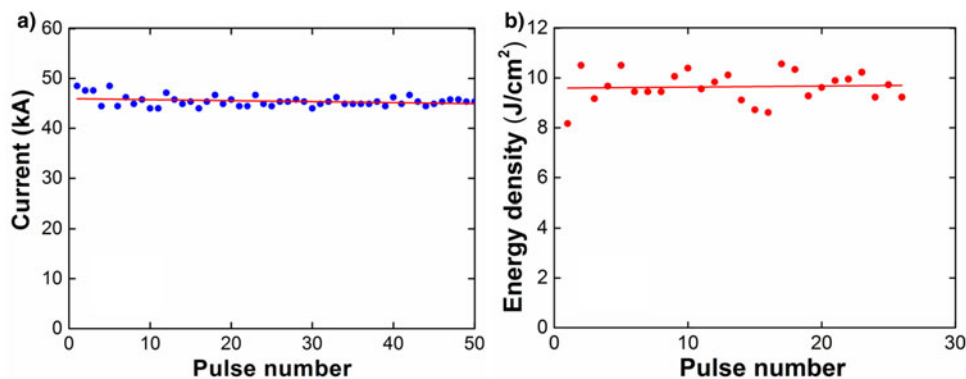

Fig. 13. Shot-to-shot variation in diode current and HIPIB energy density at a background pressure of about 10 mPa: (a) total diode current, (b) the beam energy density at the focal point.
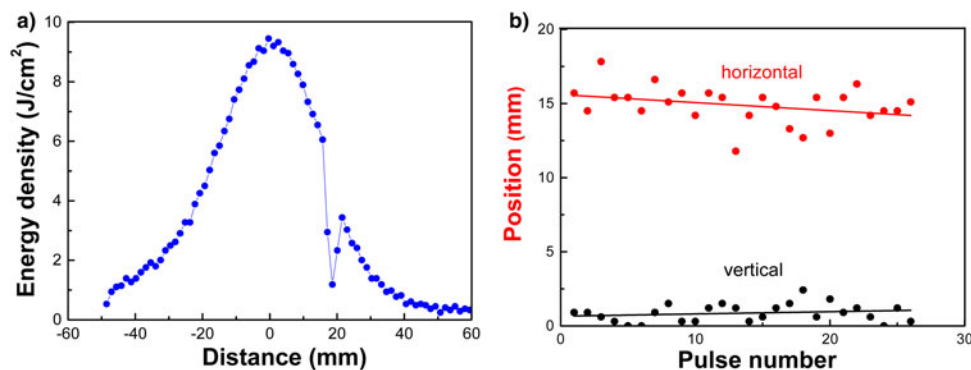

Fig. 14. Shot-to-shot variation in HIPIB deflection at the focal point under a background pressure of about 10 mPa: (a) energy density profile, (b) the ion beam deflection in both horizontal and vertical directions.

molecules within A–K gap during HIPIB generation (the second pulsed) could rise to 10^{15}–10^{16} cm^{-3} corresponding to a transient pressure of 0.3–3 Pa. Therefore, it is reasonable that increasing of background pressure in diode chamber (between pulses) to 100 mPa has little influence on the operation process of the self-magnetic field MID. It is implied that the background pressure up to 1 Pa order will not alter the plasma generation process in the A–K gap, assuming that no surface breakdown could happen in the vacuum chamber with increasing the pressure.

As for ion beam propagation in the vacuum chamber, it is found that moving of HIPIB spot center in series of pulses does not exceed ±3 mm at the considerable change of background pressure within 1–50 mPa. As the background pressure increased to a value higher than 50 mPa, it seems that a slight increase in the ion beam deflection may occur and does not exceed ±4 mm up to 90 mPa. The main mechanism for observed threshold background pressure could be occurrence of breakdown on the surface of the insulator in the diode chamber and/or the breakdown of the residual gas in the diode chamber at the pressure higher than 50 mPa. During experiments, the bright glow was observed with enhanced probability of surface breakdown in the diode chamber. In this case, the total diode current increased abruptly.

Moreover, for effective ion beam transportation, one needs to apply neutralization to create and to transport high-flux ion beams. A high ion concentration of 10^{10}–10^{13} ions cm^{-3} in the HIPIB may lead to a change in potential up to hundreds of kilovolts. As a result, the corresponding electric field causes the scattering of intense ion beam along its length (Bystritski & Didenko, 1989). For elimination of ion beam scattering one needs to reduce the beam-generated electric field by mixing low-energy electrons with the ions. The electrons should be supplied to the ion beam volume during its transportation after extracted from the A–K gap. The executed researches have shown that the increase in background pressure in diode chamber poorly change the HIPIB charging neutralization. In the ion diode acceleration of ions occurs between a layer of anode plasma and a layer of drifting electrons near a cathode surface. In the investigated diodes the drift layer thickness is 0.3–0.5 mm at A–K gap 8–9 mm, and the electron concentration in the drifting area is $(3$–$5) \cdot 10^{14}$ cm^{-3} (Pushkarev & Pak 2015). In this case, electron energy does not exceed 50 keV. With an ion current density of 100–200 A/cm^2 and accelerating voltage of 250 kV, the ion concentration in HIPIB does not exceed $5 \cdot 10^{12}$ cm^{-3} (Pushkarev et al., 2013). These ions pass through a thick layer of drifting low-energy electrons, which provides effective neutralization of the HIPIB. In summary, it is indicated that, the self-magnetic field MIDs are robust for ion beam generation and transportation at relatively wider range of vacuum condition in 1–100 mPa, and possibly higher if the electrical insulation in the diode system could be optimized. It is also partly proved by similar experimental phenomena on TEMP-4 M with different residual species with oil–vapor vacuum pump without a nitric trap, since the operation principle and anode material are the same as those on accelerator TEMP-6.

5. CONCLUSIONS

(1) HIPIB generation in the MIDs with self-magnetic field insulation using graphite anode has been investigated by controlling the residual gas pressure from 3 to 90 mPa in the diode chamber. Stable operation of the self-magnetic MIDs with repetitive ion beam output is ensured under the varied background gas pressure within 1–100 mPa.

(2) During plasma formation at anode and cathode occurs desorption of adsorbed molecules layer, the pressure in A–K gap increase up to 0.3–3 Pa. Therefore, the background pressure in diode chamber (between pulses) up to 1 Pa could not affect the working mode of the ion diode. However, slight increase in the ion beam deflection is observed at a pressure higher than 50 mPa. It is attributed to surface breakdown on the surface of the insulator and/or the breakdown of the residual gas in the diode chamber.

(3) It is found that, the ion diodes with self-magnetic field insulation may work at a moderate or even low vacuum condition if the breakdown in the diode system could be eliminated by optimized insulation design. Therefore, stable ion beam generation is feasible by using inexpensive and simple vacuum equipment for HIPIB generation; and moreover, the ion diodes with graphite anode as ion supply have long lifetime more than 10^6 pulses with relatively stable HIPIB generation, making their perspective for various technological applications.

REFERENCES

BYSTRITSKI, V.M. & DIDENKO, A.N. (1989). *High-Power Ion Beams*. New York: American Institute of Physics.

CHERNOV, I.P., BEREZNEEVA, E.V., BELOGLAZOVA, P.A., IVANOVA, S.V., KIREEVA, I.V., LIDER, A.M., REMNEV, G.E., PUSHILINA, N.S. & CHERDANTSEV, YU.P. (2014). Physicomechanical properties of the surface of a zirconium alloy modified by a pulsed ion beam. *Tech. Phys.* **59**, 535–539.

DAVIS, H.A., BARTSCH, R.R., OLSON, J.C., REJ, D.J. & WAGANAAR, W.J. (1997). Intense ion beam optimization and characterization with infrared imaging. *J. Appl. Phys.* **82**, 3223–3231.

Davis, H.A., Remnev, G.E., Stinnett, R.W. & Yatsui, K. (1996). Intense ion-beam treatment of materials. *MRS Bull.* **21**, 58–62.

Langmuir, I. (1913). The effect of space charge and residual gases on thermionic currents in high vacuum. *Phys. Rev.* **2**, 45–51.

Lei, M.K., Zhu, X.P. & Guo, D.M. (2016). Reducing geometrical, physical and chemical constraints in surface integrity of high performance stainless steel components by surface modification. *J. Manuf. Sci. Eng. –Trans. ASME* **138**, 044501.

Lei, M.K., Zhu, X.P., Liu, C., Xin, J.P., Han, X.G., Li, P., Dong, Z.H., Wang, X. & Miao, S.M. (2009). A novel shock processing by high-intensity pulsed ion beam. *J. Manuf. Sci. Eng. – Trans. ASME* **131**, 031013.

Lei, M.K., Zhu, X.P. & Wang, X.J. (2002). The oxidation resistance of ion-implanted γ-TiAl base intermetallics. *Oxid. Met.* **58**, 361–374.

Olson, C.L. (1982). Ion beam propagation and focusing. *J. Fusion Energy* **1**, 309–339.

Pointon, T.D. (1989). Charge exchange effects in ion diodes. *J. Appl. Phys.* **66**, 2879–2887.

Pushkarev, A.I., Isakova, Yu.I. & Khailov, I.P. (2013). The influence of a shield on intense ion beam transportation. *Laser Part. Beams* **31**, 493–501.

Pushkarev, A.I., Isakova, Yu.I. & Khailov, I.P. (2014). Correlation analysis of intense ion beam energy in a self magnetically insulated diode. *Laser Part. Beams* **32**, 311–319.

Pushkarev, A.I., Isakova, Yu.I. & Khailov, I.P. (2015). Intense ion beam generation in a diode with explosive emission cathode in self-magnetically insulated mode. *Euro. Phys. J. D: Plasma Phys.* **69**, 40. https://doi.org/10.1140/epjd/e2014-50319-8.

Pushkarev, A.I. & Pak, V.G. (2015). Analysis of drifting electron concentration in a self-magnetically insulated ion diode. *Tech. Phys. Lett.* **41**, 146–148.

Remnev, G.E., Uglov, V.V., Shymanski, V.I., Pavlov, S.K. & Kuleshov, A.K. (2014). Formation of nanoscale carbon structures in the surface layer of metals under the impact of high intensity ion beam. *Appl. Surf. Sci.* **310**, 204–209.

Renk, T.J., Provencio, P.P., Prasad, S.V., Shlapakovski, A.S., Petrov, A.V., Yatsui, K., Jiang, W. & Suematsu, H. (2004). Material modifications using intense ion beams. *Proc. IEEE* **92**, 1057–1081.

Renk, T.J., Sridharan, K., Harrington, S.P., Johnson, A.K. & Lahoda, E. (2010). Incorporation of gadolinium and boron into Zirconium alloy: Surface alloying of immiscible materials using an intense pulsed ion beam. *Nucl. Instrum. Methods Phys. Res. B* **268**, 2666–2678.

Rej, D.J., Bartsch, R.R., Davis, H.A., Faehl, R.J., Greenly, J.B. & Waganaar, W.J. (1993). Microsecond pulse width, intense, light-ion beam accelerator. *Rev. Sci. Instrum.* **64**, 2753–2760.

Rej, D.J., Davis, H.A., Olson, J.C., Remnev, G.E., Zakoutaev, A.N., Ryzhkov, V.A., Struts, V.K., Isakov, I.F., Shulov, V.A., Nochevnaya, N.A., Stinnett, R.W., Neau, E.L., Yatsui, K. & Jiang, W. (1997). Materials processing with intense pulsed ion beams. *J. Vac. Sci. Technol. A* **15**, 1089–1097.

Rose, D.V., Ottinger, P.F., Welch, D.R., Oliver, B.V. & Olson, C.L. (1999). Numerical simulations of self-pinched transport of intense ion beams in low-pressure gases. *Phys. Plasmas* **6**, 4094–4103.

Stepanov, A.V., Lopatin, V.S., Remnev, G.E. & Melnikova, E.N. (2008). Repetitive rate operation mode of magnetically isolated diode with dielectric anode. *15th Int. Symp. on High–Current Electronics: Proc. Tomsk: Publish House of the IAO SB RAS*, 100–102.

Suematsu, H., Kitajima, K., Suzuki, T., Jiang, W., Yatsui, K., Kurashima, K. & Bando, Y. (2002). Preparation of polycrystalline boron carbide thin films at room temperature by pulsed ion-beam evaporation. *Appl. Phys. Lett.* **80**, 1153–1155.

Werner, Z., Piekoszewski, J. & Szymczyk, W. (2001). Generation of high-intensity pulsed ion and plasma beams for material processing. *Vacuum* **63**, 701–708.

Zhu, X.P., Lei, M.K. & Ma, T.C. (2002). Characterization of a high-intensity bipolar-mode pulsed ion source for surface modification of materials. *Rev. Sci. Instrum.* **73**, 1728–1733.

Zhu, X.P., Suematsu, H., Jiang, W. & Yatsui, K. (2008). Structures and photoluminescence properties of silicon thin films prepared by pulsed ion-beam evaporation. *Mater. Sci. Eng. B* **149**, 105–110.

Zhu, X.P., Zhang, F.G., Song, T.K. & Lei, M.K. (2014). Nonlinear wear response of WC-Ni cemented carbides irradiated by high-intensity pulsed ion beam. *J. Tribol. –Trans. ASME* **136**, 011603.

Zhu, X.P., Zhang, F.G., Tang, Y. & Lei, M.K. (2011). Phase transformation under beam-target interactions during high-intensity pulsed ion beam irradiation at low pressure. *Laser Part. Beams* **29**, 283–289.